

POLITECNICO DI TORINO

Mechanical Engineering



**Politecnico
di Torino**

Master's degree thesis

Warm forming processes for high-performance aluminum alloys for the automotive industry

Supervisors

Prof. MATTEIS Paolo

Prof. UBERTALLI Graziano

Candidate

CHEN Minye

December 2021

Abstract

A summary and description of the current automotive applications of aluminum alloys, heat treatment methods, and problems that may be encountered in warm forming are presented. A series of warm forming tests were carried out on the problem of generally low formability of aluminum alloys at room temperature. The mechanical properties of AA5083 and AA7046-T6 were studied and analyzed at different temperatures and tensile speeds in an attempt to find the best warm forming solution. The experiments showed that the hardness of both aluminum alloys was very slightly affected at the test temperature of this warm forming, and AA7046 had more sensitive warm forming properties.

Key words: lightweight, aluminum alloy 5083, aluminum alloy 7046, warm forming

Acknowledgements

I am very grateful to Prof. MATTEIS Paolo and Prof. UBERTALLI Graziano for their help and for their patience and expertise that enabled me to carry out and complete my thesis work. I would also like to thank my family and friends for their support along the way.

Index

1. Introduction	6
1.1 Classification of automotive lightweighting technologies	7
1.2 Advantages of choosing aluminum alloy	8
1.3 Aluminum alloy series commonly used in the automotive industry	11
2. Heat treatment of aluminum alloys	12
2.1 The purpose of heat treatment	12
2.2 Heat treatment methods	13
3. Aluminum alloy surface treatment processes	14
4. Warm forming	15
4.1 What is warm forming?	15
4.2 Why to use warm forming	16
4.3 Nonisothermal warm forming	19
4.4 The effect of temperature on springback	22
4.5 Relationship between LDR (Limiting draw ratio) and punch velocity	24
4.6 Possible defects of warm forming	25
4.7 Lubrication	27
5. Experiments and results	30
5.1 Materials	30
5.2 Heat treatment	32
5.3 Tensile tests	33
5.31 Experimental procedures	33
5.32 Tensile test results for AA5083	35
5.33 Tensile test results for AA7046	39

5.34 Observations for broken samples.....	42
5.4 Optical Metallography.....	45
5.41 Samples preparation.....	45
5.42 Microstruture analysis.....	47
5.5 Microhardness tests.....	50
5.51 Equipment and principle.....	50
5.52 Data analysis.....	52
6. Conclusions.....	53
7. Appendix I.....	55
8. References.....	64

1. Introduction

With the continuous development of automobile industry, the number of automobiles has increased dramatically, and there are more than 1 billion automobiles worldwide[31]. The automobile has become one of the most important sources of energy consumption and pollutant emissions in the world, which has a huge impact on ecology and resources. Currently, all major countries in the world have enacted strict policies to limit fuel consumption and carbon emissions from automobiles. In order to save energy, reduce fuel consumption, reduce exhaust emissions and achieve sustainable development, automobile manufacturers take many measures, one of the most effective measures is to reduce the mass of the car without reducing services. Some relevant data show that for every 10% reduction in vehicle mass, fuel efficiency can be increased by 6% ~ 8% [1], in addition, the realization of lightweight cars is also conducive to improving the power, comfort and handling stability of the car.

1.1 Classification of automotive lightweighting technologies

Automotive lightweighting technology can be divided into three main aspects: optimized structural design, application of lightweight materials, and advanced manufacturing process.

- The optimized structural design includes: size optimization, shape optimization, topology optimization and multidisciplinary design optimization of automotive structures.

- The application of lightweight materials includes: high-strength steel, aluminum alloy, magnesium alloy, plastic and composite materials, etc.

- Advanced manufacturing processes include: hydroforming and laser welding, etc.

1.2 Advantages of choosing aluminum alloy

In the automotive field, the light weight materials used are mostly light alloy materials, of which aluminum alloys are typical. Compared with carbon fiber reinforced plastics (CFRPs), aluminum alloys are less expensive. In addition, aluminum alloys are less in density, only 1/3 of steel, and some studies have shown that significant weight reduction can be achieved when replacing mild steel, cast iron, or high-strength steel with aluminum alloys, while some studies have shown that each kilogram of aluminum replacing mild steel, cast iron, or high-strength steel can reduce greenhouse gas emissions by 13-20 kg under standard conditions for the whole vehicle life [2]. In addition, compared with steel materials, aluminum alloys also have the advantages of high thermal conductivity, corrosion resistance, and good processing performance, which are excellent lightweight materials with relatively early application and mature technology[3] ;

Series	Cast aluminium alloy composition	Wrought aluminium alloy composition
1	Al	Al
2	Al+Cu	Al+Cu
3	Al+Si+Cu/Mg	Al+Mn
4	Al+Si	Al+Si
5	Al+Mg	Al+Mg
6	Al+Zn	Al+Mg+Si
7	Al+Mg+Zn	Al+Mg+Zn
8	Al+Sn	Al+Li/Sn/B

Table 1: Aluminium Alloy Series Composition[17]

At present, aluminum alloys for automobiles are mainly cast aluminum, wrought aluminum, aluminum plates and aluminum profiles. With the development and application of new materials such as fast-solidified aluminum alloys, powder metallurgy aluminum alloys, superplastic aluminum alloys, aluminum matrix

composites and foam aluminum, the application of aluminum alloys in automobiles will be further expanded in the future. At present, aluminum alloys used in automobiles are mainly cast components of aluminum, accounting for about 80% of the aluminum used in automobiles, mainly used in the manufacture of engine parts, shell parts and other parts of the chassis. Now they have been applied in large quantities of parts are engine block, cylinder head, clutch housing, bumper, wheels, engine bracket and other parts. However forged aluminum has better mechanical properties and is also used in automobiles, such as forged aluminum wheels.

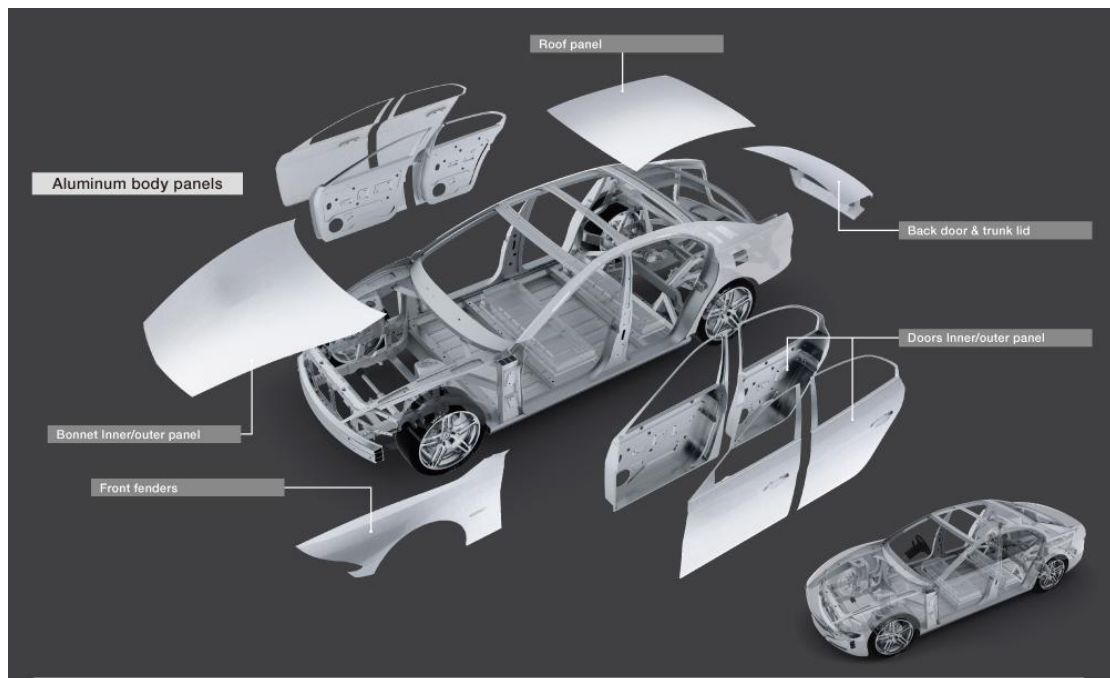


Fig. 1: Use of Aluminum Alloys in Automobiles[4]

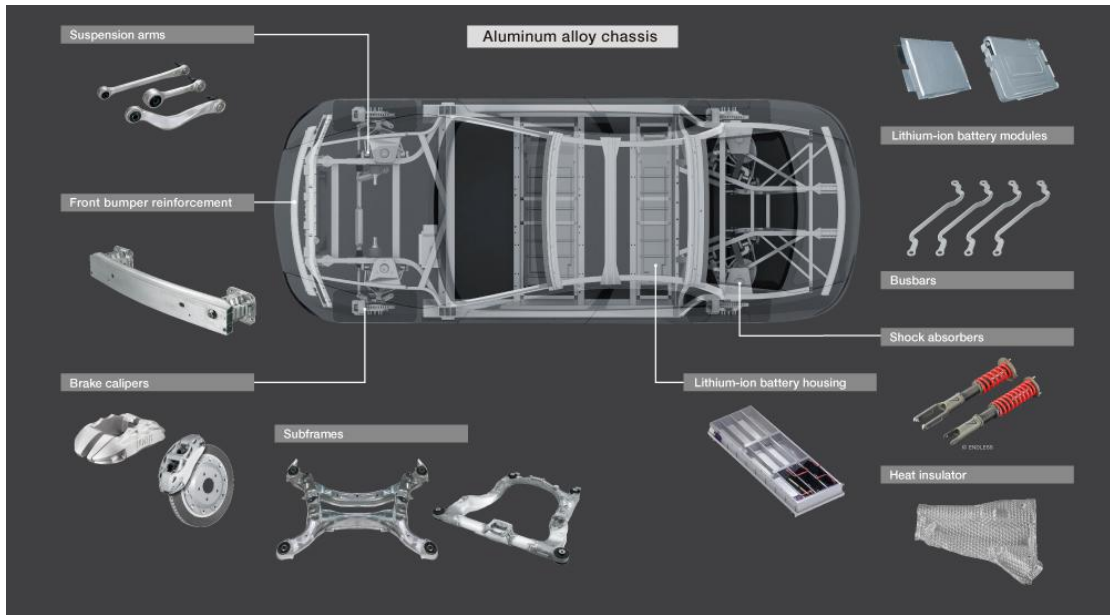


Fig. 2: Use of Aluminum Alloys in Automobiles[4]

1.3 Aluminum alloy series commonly used in the automotive industry

They mainly include 3000 series, 5000 series, 6000 series, 7000 series alloy plates, profiles, tubes and high-performance cast aluminum, and different types of aluminum alloy materials are used for different stress parts.

3xxx aluminum alloy: with Mn as the main alloying element. moderate strength, good corrosion resistance, good formability, suitable for use at high temperatures. They are the main components of today's automotive heat exchangers [16].

5xxx aluminum alloy: with Mg as the main element, it can also be called aluminum-magnesium alloy, which has good formability, corrosion resistance and welding properties [6]. However, the annealed state may produce Lüders line and delayed yielding during processing deformation, so it is mainly used for complex shape parts such as inner body panels.

6xxx aluminum alloy: Mg, Si are the main alloying elements and some contain Cu, which are heat treatable and strengthenable aluminum alloys with medium strength, good plasticity and excellent corrosion resistance [5]. At present, 6009, 6010 and 6016 aluminum alloys are used in the outer and inner panels of automobile bodies because of their characteristics such as good plasticity and the possibility of artificial aging to obtain higher strength during the painting and baking process after forming.

7xxx aluminum alloys: Mg, Zn are the main alloying elements and also contain Cu. They have low density, high strength, high toughness, excellent heat resistance, fatigue resistance, corrosion resistance[5]. Currently, most major automotive suppliers are developing 7xxx sheet alloys for vehicles, making it one of the hot spots for the development of lightweight structural materials. It is mainly used for the body skeleton, the most stressed part of the body.

2. Heat treatment of aluminum alloys

2.1 The purpose of heat treatment

The purpose of heat treatment of aluminum alloy is to improve the mechanical properties and corrosion resistance, stabilize the size, and improve the machining properties such as cutting and welding. Specifically, the following aspects:

- 1) To eliminate the internal stress caused by uneven cooling rate during crystallization and solidification of the casting , due to the structure of the casting (such as uneven thickness of the wall, thick at the joints).
- 2) Improve the mechanical strength and hardness of the alloy, improve the microstructure, to ensure that the alloy has a certain degree of plasticity and cutting performance, welding performance.
- 3) Stabilize the size of the casting to prevent and eliminate high temperature phase changes that cause volume changes.
- 4) Eliminate intergranular and compositional segregation to homogenize the material.

2.2 Heat treatment methods

Annealing: The product is heated to a temperature and kept warm for a period of time and then cooled to room temperature at a certain cooling rate to make the microstructure more uniform and stable through atomic diffusion migration, so as to eliminate the internal stress of the casting and achieve the purpose of improving plasticity, reducing deformation and warpage.

Solution and quenching: Heat treatment of aluminum alloy materials that can be strengthened to a higher temperature and maintained for a period of time, so that the second phase or other soluble components in the material fully dissolved in the aluminum matrix, and then fast cooling to room temperature, it is an unstable state, because in the high-energy state, solute atoms at any time there is the possibility of precipitation. However, the plasticity of the material is high at this time and can be subjected to cold working or straightening processes [7].

Aging: After solution quenching, the material is kept at room temperature or a higher temperature for a period of time, and finally air-cooled until room temperature, so that the unstable supersaturated solid solution decomposes, and metastable second phase particles will precipitate from the supersaturated solid solution, distributed in the aluminum grains, so that the alloy microstructure is more stable, thus producing a strengthening effect called precipitation strengthening.

Natural aging: Some alloys (such as 2024, etc.) can produce precipitation strengthening at room temperature, called natural aging.

Artificial aging: Some alloys (such as 7075, etc.) at room temperature, the precipitation strengthening is not obvious, while the precipitation strengthening effect at higher temperatures is obvious, called artificial aging.

3. Aluminum alloy surface treatment processes

Usually, a thin oxide film will be formed on the surface of aluminum alloy, which will give the aluminum alloy at certain corrosion resistance, but this is far from enough, so we usually need to use the relevant surface treatment process to increase the thickness of its protective film, so as to reduce or protect it from the erosion of external environmental factors and thus increase its service life [8]. The main surface treatment processes used are as follows:

Chemical oxidation: the use of chemical oxidizers (bichromate, permanganate, etc.) to generate oxide films is the most traditional oxidation method, which has the advantages of being economical, fast and simple, and is suitable for the low-cost production of high-volume parts [9].

Anodic oxidation: Placing aluminum and its alloys in a suitable electrolyte as an anode for electrification, it is the most commonly used surface treatment of aluminum alloys in the world today. However, according to studies in recent years, some of the chemical oxidizers produce harmful gases in the processing and production, which are carcinogenic risks. Example include chromic acid [10].

Microarc oxidation: It is a new treatment process to grow ceramic film on the surface of aluminum alloy (e.g. MOCVD, MBE, laser deposition, and magnetron sputtering [11] [12] [13] [14]), and the oxide film has high hardness properties, which makes the aluminum alloy more corrosion resistant, impact resistant, and insulating [15].

4. Warm forming

4.1 What is warm forming?

Metals are deformed by heating them to a temperature that maximizes their malleability without allowing them to re-crystallize, grow grains, or fracture. The process allows the part to be successfully formed with net shape features and to final tolerance that eliminate secondary machining operations. Tolerances, material, shape and final specifications determine the optimum temperature for a given part[20].

4.2 Why to use warm forming

Since aluminum has lower formability and Young's modulus than steel, which will lead to more wrinkling and springback[18], the use of warm forming techniques can significantly improve the formability of aluminum. Interest in warm forming of lightweight materials began in the 1970s when it was found that an aluminum alloy with 6% magnesium content could achieve 300% total elongation at approximately 250 °C.

In warm forming of aluminum, molds and blank supports are typically heated to a range of 150 to 300 degrees Celsius. The mold and the blank holder are heated with an electric heating rod located in the mold. It is necessary to heat the corners of the mold, because the corners are the key to control the metal flow. Therefore, in most cases, it is not necessary to heat the entire mold. Straight sides can be cooled by using water or oil. This reduces the material flow, similar to the effect of draw bead [18].

Many studies have shown a significant improvement in the formability of the 5xxx and 6xxx series when warm forming is used [18] [19]. For example, Bolt performed an experimental analysis of rectangular cups of aluminum alloy deep drawn at room temperature (20 °C), 100 °C, 175 °C and 250 °C. The device used is a hydraulic press with a punch, die, and blankholder modified to apply a warm forming test at 1000 kN, with a punch speed of 120 mm/min. The punch clearance is 1.5 mm, the radius of the punch is 10 mm, and the draw-in radius of the die is 8 mm. It is used for drawing non-rectangular blanks of 210 mm in length, 130 mm in width and 30 mm in corner radius.

The four corners of the die and blankholder could be heated by electric heaters, but no additional cooling was applied to the straight sides. The maximum achievable die temperature was 250°C and the punch was kept at room temperature (20°C) by water cooling. The materials tested were 1.15 mm thick 6016-T4, 1.20 mm thick 5754-O

and 1.0 mm thick 1050-H14. In order to maintain its lubricity at the test temperature, both sides of the blanks were lubricated with a lubricant (Petrofer Isoform WP.5).

The heating had the effect of softening the material between the die and the blankholder and near the draw-in radius, reducing the forces required for flange deformation. Fig. 5 and Fig. 6. The results indicate that the ultimate height of the final product for all materials deep drawn at 175°C is 20-25% higher than at room temperature. For alloys 1050-H14 and 6016-T4, an increase in deep drawing rate is observed at all elevated temperatures.

However, for alloy 5754-O, an increase in drawability was observed only at the test temperature of 175°C. At 100°C, the drawability seems to decrease slightly. In addition, wrinkling of flange is significantly reduced at the highest test temperature of 175°C.

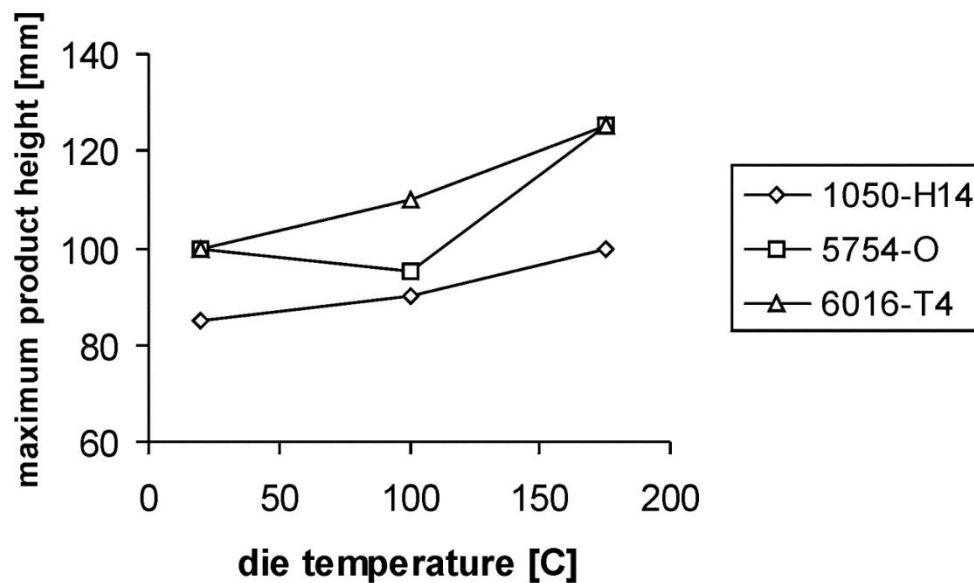


Fig. 5: Effect of the die temperature on the maximum achievable product height of a rectangular box shape. The initial blankholder pressure was 0.5, 2 and 1 MPa for 1050-H14, 5754-O and 6016-T4, respectively

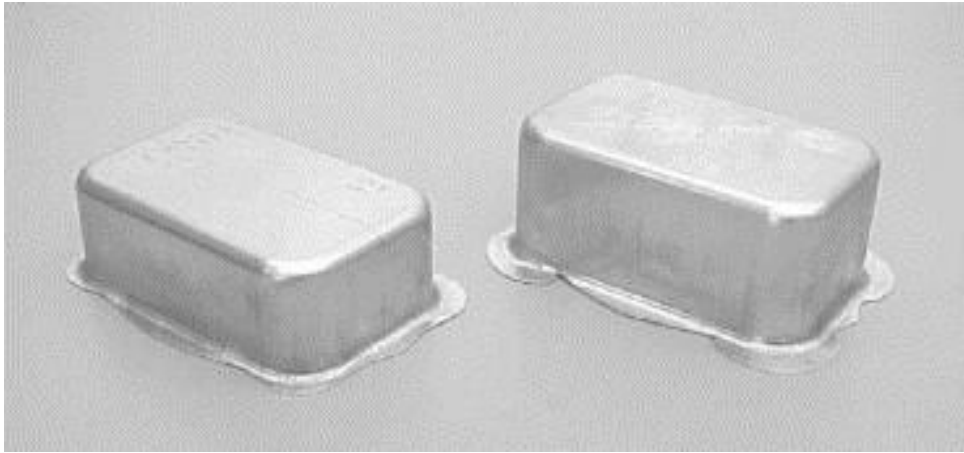


Fig. 6: Deepest box shaped product of 1050-H14 aluminium drawn at room temperature (left) with a 80 mm product height blank and at 175°C (right) with a 100 mm product height blank; initial blankholder pressure was 0.5 MPa

4.3 Nonisothermal warm forming

According to relevant studies, the punch temperature has a considerable influence on the limitation of aluminum warm forming process. The experiments were carried out using a 100 mm diameter punch for deep drawing ($V_{st}=5$ mm/s, lubricant: B 393 G) of 1.0 mm and 1.3 mm magnesium alloy plate, 1.0 mm aluminum plate at different heating temperatures. However, the LDR was affected by the gradual increase in punch temperature due to the heat transfer occurring in the heated balnkholder. The results showed that the increase in punch temperature would lead to a decrease in the achievable limiting draw rate due to the low transferable drawing force (Fig. 7).

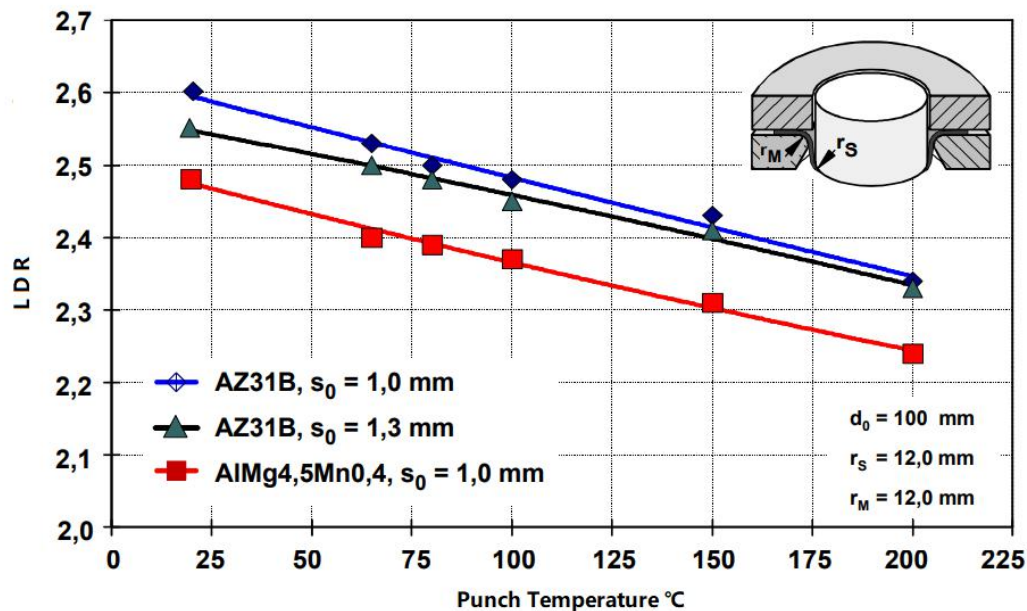


Fig. 7: The Limiting draw rate (LDR) relationship with increase in punch temperature [22].

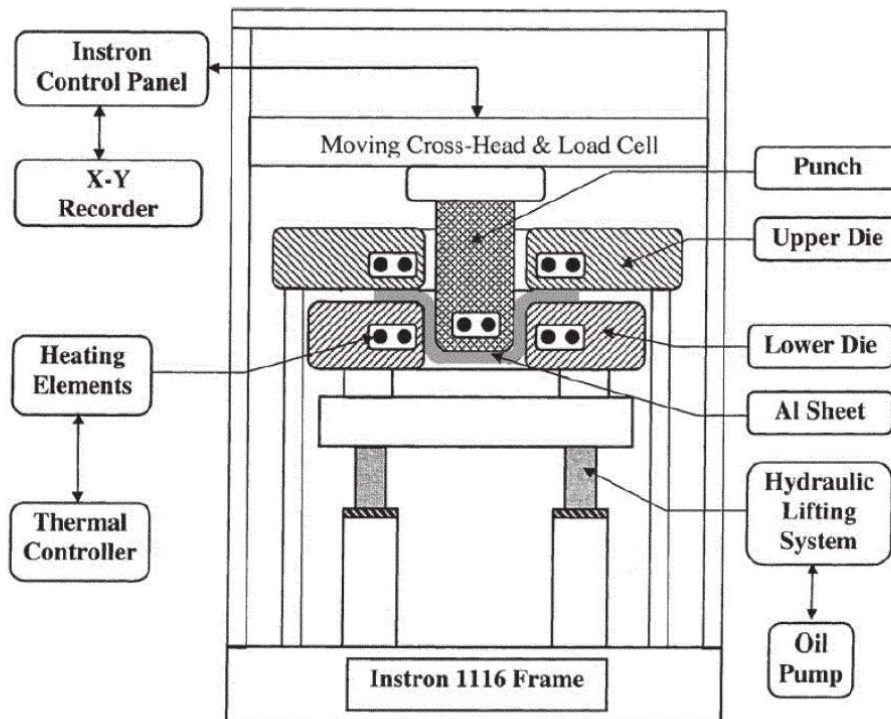


Fig. 8: Schematic diagram of the die where the die and punch are heated [23].

In order to provide more formability, punches need to have an additional cooling control device. In Fig. 9, a schematic diagram of a deep drawn plate divided into five deformation zones (A-B, B-C, C-D, D-E, E-F) shows the heating and cooling of the different zones [21]. The blank (E-F) must be heated, which means the blankholder and the die are heated to reduce the compressive stress in the flange area and to promote metal flow. However, once the sheet enters and starts to contact the punch walls (D-C) and the corners of the punch (C-B), the sheet temperature drops through heat transfer to the water-cooled punch, which means that it can withstand more tensile stress and therefore stretch less, reducing the possibility of fracture and thus allowing it to draw smoothly into the die cavity. However, the sheet under a heated die has a higher temperature, which is necessary for forming at the corners of the die (E-D).

In addition, additional cooling equipment can increase production costs. The choice of

nonisothermal tooling depends on the degree of increased formability of the aluminum alloy required.

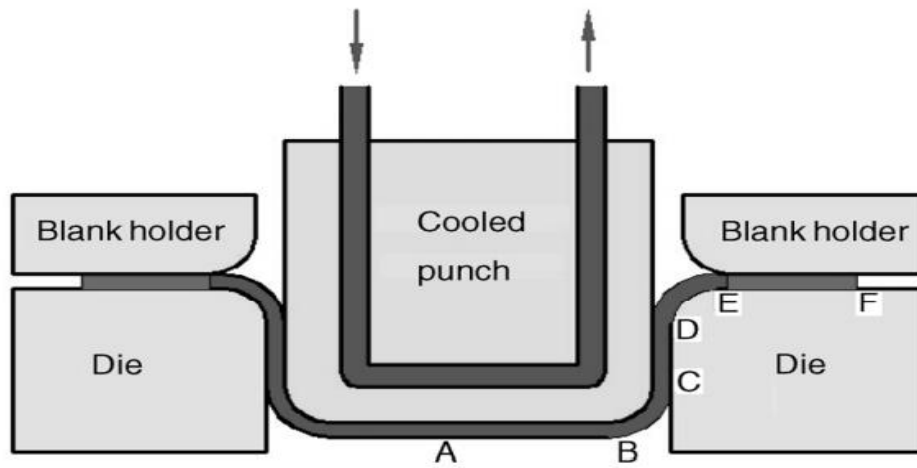


Fig. 9: In nonisothermal warm forming, cooling the die corner and the punch increases drawability[21].

4.4 The effect of temperature on springback

After bending the metal sheet, a part of the material in the bending deformation area undergoes plastic deformation and the other part only experiences elastic deformation. The elastic deformation of the material needs to be restored to its original state due to unloading of the press, resulting in the sheet springing back. Therefore, the elastic deformation of the material plays an important role in the springback. Laurent et al. used 1 mm thick AA5754-O sheet and deep-drew it to a height of 60 mm at temperatures of 25°C, 100°C, 150°C, and 200°C respectively. The stretched sheet became thinner (between 0.95 mm and 1 mm in thickness) between a height of 5 mm and 25 mm, 25 mm to 60 mm becomes thicker (above 1 mm) [30]. The height was taken and cut at 20 mm mm from the bottom to make a cup shape ($d = 100$ mm), and then a second cut was made at 15 mm from the bottom of the cup to make a ring with a height of 5 mm.

Subsequent cutting of the rings showed that the opening gap decreased from about 65 mm (25°C) to about 21 mm (200°C), and the data are shown in Table 2. Also, the trend of decreasing springback with increasing temperature can be clearly observed from Fig. 10.



Fig. 10: Opening of the rings for several temperatures in the range 25–200°C.

Temperature (°C)	25	100	150	200
Experimental opening (mm)	64	51	37	21
Numerical opening (mm)	65	56.2	46	27.6

Table 2: Experimental and numerical opening of the ring as a function of temperature.

4.5 Relationship between LDR (Limiting draw ratio) and punch velocity

Kaya et al. conducted experiments [25] using Nonisothermal Deep Drawing to study the variation of LDR versus punch speed for the same size aluminum 5754-O sheet (112 mm diameter and 1 mm thickness) at three different forming temperatures of 250°C, 275°C, and 300°C, respectively (all heating times were 90 s). In Fig. 11, it can be easily found that the LDR tends to decrease with increasing punch velocity in all temperature cases. Also, increasing the temperature can use faster punch velocity while obtaining the same LDR.

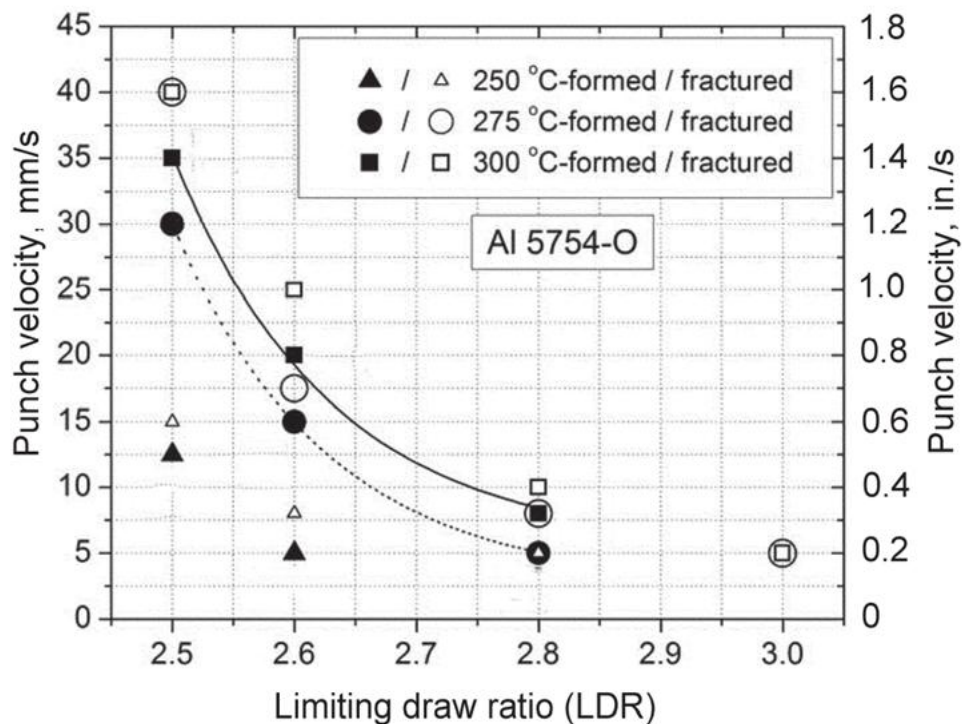


Fig. 11: Relationship between LDR and Punch velocity for aluminum 5754-O alloy[25].

4.6 Possible defects of warm forming

Fig. 12 shows possible forming defects (early fracture, wrinkling, uneven sheet flow) in warm forming of an aluminum alloy [26]. Figure (a) shows early fracture due to insufficient flange temperature and/or excessive blank clamping force. This means that the sheet temperature at the flange is not high enough to facilitate pulling into the die cavity. In addition, the blank clamping force should be high enough to prevent wrinkling during deep drawing (Figure b). Insufficient cooling of the punch can lead to fracture (Figure c) because the drawing stress that the cup wall can withstand decreases as the temperature increases. This problem can sometimes be eliminated by drawing at a slower punch speed so that the sheet can cool down through contact with the punch. A higher LDR can be obtained with warm deep drawing compared to conventional deep drawing at room temperature (Fig. d).

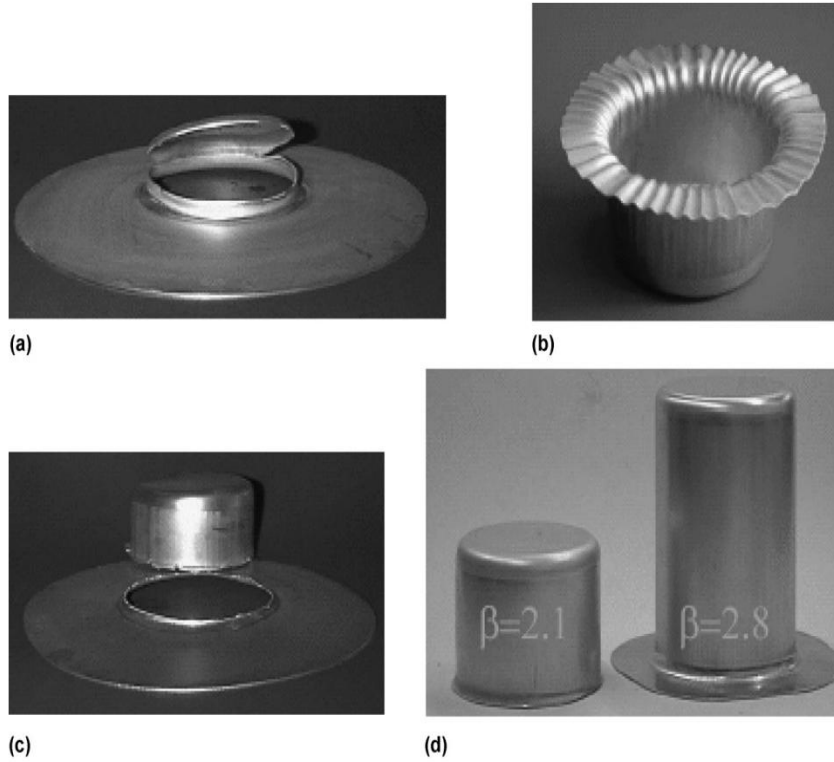


Fig. 12: Possible defects and successfully drawn cups in warm deep drawing. (a) Fracture due to insufficient flange temperature and/or excessive blank holder force. (b) Wrinkling due to low blank holder force. (c) Fracture due to insufficient punch cooling. (d) Cold deep drawing: limiting draw ratio (LDR) = 2.1. Warm deep drawing with partial cooling: LDR = 2.8 [26].

4.7 Lubrication

The use of correct lubrication conditions is necessary to reduce part-tools wear during machining. In particular, lubrication is more important in warm forming than in room temperature forming, because temperature changes the properties of the lubricant and increases the tendency for galling. A good quality lubricant must meet the following standards:

- Good lubrication.
- High temperature stability.
- Non-toxic
- Good adhesion
- Easy to apply
- Easy to remove
- Low cost

Maillard et al. used 0.8 mm thick AW-5083 H111 (EN 485-2) aluminum alloy and progressive die to simulate a number of relevant tests (Table 2) using several different lubrication methods during warm forming at 180°C [27]. The final check of the tools (blank holders and die radius) and parts (proportion below the blank holder and rubbing portion over the die radius) for the presence of marks, scratches or picks, as well as the residue of the blankholder lubricant was used to determine the effects.

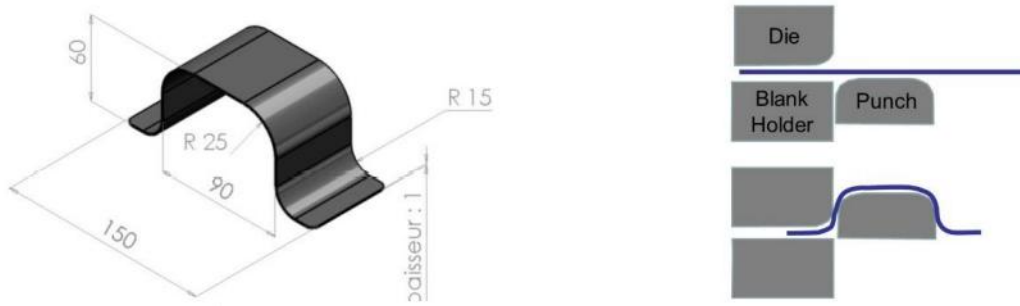


Fig. 13: Shape of the channel part and punch, die and blank holder.

Material / surface coating	Lubricant	Configuration
X153CrMoV12 (without coating)	IN 1514	Oil based 1
	O WD (13%)	Water based 2
X153CrMoV12 / CrN + a-C:H (with coating)	IN 1514	3
	O WD (13%)	4

Table 2: Parameters of the configurations tested during the tests.

From the results of Table 3, all the test configurations have good lubrication conditions, and no lubricant residue was found in Configuration 2 with OWD water-based lubricant alone, while residue was found in Configuration 1 with oil-based lubricant alone but not in Configuration 3, the lubricant residue is probably due to the role of the coating on the tool. The combination of coating and lubricant performed better in terms of residues, but the configuration with lubricant alone showed a lower risk of galling and no pick up marks were produced. In addition, the configuration using only lubricant alone would have better economic benefits in industrial production.

Test config.	Part		Tool	
	Portion rubbing against the die radius	Portion below the blank holder	Blank holder	Die radius
1	No significant damage. Presence of friction marks which cannot be felt by touch.	No marks or scratches.	Small quantity of lubricant residues outside the area in contact with the sheet.	No pick-up.
2	No significant damage. Presence of friction marks which cannot be felt by touch.	Scratches and pronounced marks.	No lubricant residues.	No pick-up.
3	No significant damage. Presence of friction marks which cannot be felt by touch.	No marks or scratches.	Pick-up. No lubricant residues.	No pick-up.
4	Light degradation of the surface of the part with presence of slightly scratched "whitened" areas.	No marks or scratches.	No lubricant residues.	Pick-up.

Table 3: Summary of the examination of the parts and tools after the tests.

5. Experiments and results

5.1 Materials

In order to study the formability of aluminum alloys, the materials selected for testing are the aluminum alloys 5083 and 7046 from Fig. 14. 12 "dog bone" shape specimens of alloy 5083 and 8 specimens of alloy 7046. The chemical composition of the alloy is given in Table 4.

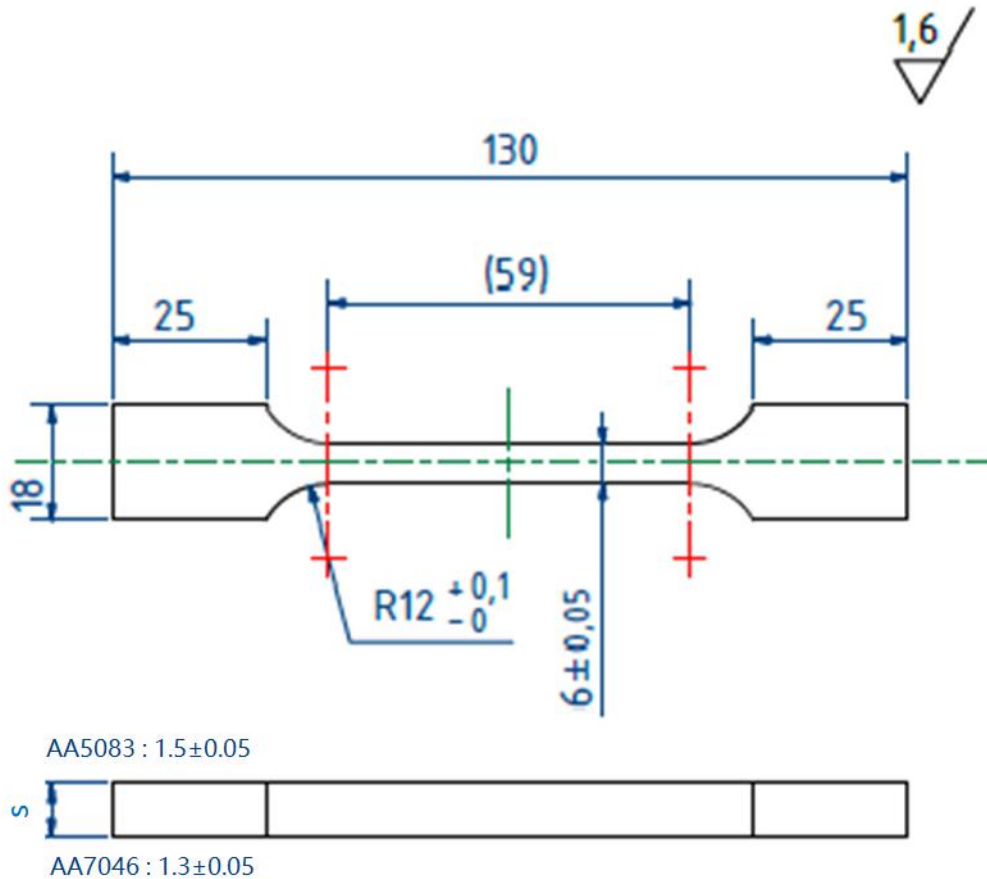


Fig. 14: Dimension of the specimen

AA5083 Physical Properties	
Density	<u>2.66</u> g/cc
Component Elements	
Aluminum, Al	92.4 - 95.6 %
Chromium, Cr	0.05 - 0.25 %
Copper, Cu	<= 0.10 %
Iron, Fe	<= 0.40 %
Magnesium, Mg	4.0 - 4.9 %
Manganese, Mn	0.40 - 1.0 %
Other, each	<= 0.05 %
Other, total	<= 0.15 %
Silicon, Si	<= 0.40 %
Titanium, Ti	<= 0.15 %
Zinc, Zn	<= 0.25 %

AA7046 Physical Properties	
Density	<u>2.82</u> g/cc
Component Elements	
Aluminum, Al	89 - 92.3 %
Chromium, Cr	<= 0.20 %
Copper, Cu	<= 0.25 %
Iron, Fe	<= 0.40 %
Magnesium, Mg	1.0 - 1.6 %
Manganese, Mn	<= 0.30 %
Other, each	<= 0.05 %
Other, total	<= 0.15 %
Silicon, Si	<= 0.20 %
Titanium, Ti	<= 0.06 %
Zinc, Zn	6.6 - 7.6 %
Zirconium, Zr	0.10 - 0.18 %

Table 4: 5083, 7046 Aluminum Composition Spec[29].

5.2 Heat treatment

We performed heat treatment on only 8 experimental samples of AA7046, in the following sequence:

- Solubilization at 480 °C for 2 hours (Experimental equipment: FURNACE TYPE IONOS 501 WITH MAXIMUM TEMPERATURE 1200°C), followed by immediate water quenching in a water-filled basin.
- Partial aging at 100 °C in boiling water for 20 min.

5.3 Tensile tests

5.3.1 Experimental procedures

The tensile test was conducted on a Zwick-Roell Z050 TH universal tensile tester (Fig. 15). First, the range, load, stretching speed and other parameters are set in the measurement program; then, the specimen is installed and the extensometer is placed, and the calibration of load, deformation and displacement are cleared; finally, the specimen is tested, the data is output, and the specimen is removed after it is fractured. In addition, the test at high temperature is performed in a high-temperature furnace (Fig. 16), which can quickly heat the sample to the target temperature.



Fig. 15: Zwick-Roell Z050 TH Universal Tensile Tester



Fig. 16: Internal details of the high-temperature furnace

5.32 Tensile test results for AA5083

A total of 12 tensile tests were performed on sample AA5083 at different temperatures and crosshead speeds (stress-strain relationship Fig. 17, relevant data Table 5).

- 2 tests at RT and 10 mm/min
- 2 tests at 200 °C and 10 mm/min
- 2 tests at RT and 600 mm/min
- 2 tests at 200 °C and 600 mm/min
- 2 tests at 120°C and 10 mm/min
- 2 tests at 150°C and 10 mm/min

Alloy 5083 (Average Value)	Ultimate Tensile Strength (MPa)	Yield Strength (MPa)	Uniform Elongation (%)	Elongation At Fracture (%)
RT 10mm/min	445	353	6.9	7.4
RT 600mm/min	450	364	5.0	5.0
120°C 10mm/min	445	377	6.0	6.4
150°C 10mm/min	413	355	4.7	6.6
200°C 10mm/min	371	332	2.5	6.5
200°C 600mm/min	409	358	3.0	3.1

Table 5: Main data of AA5083 stress-strain curves

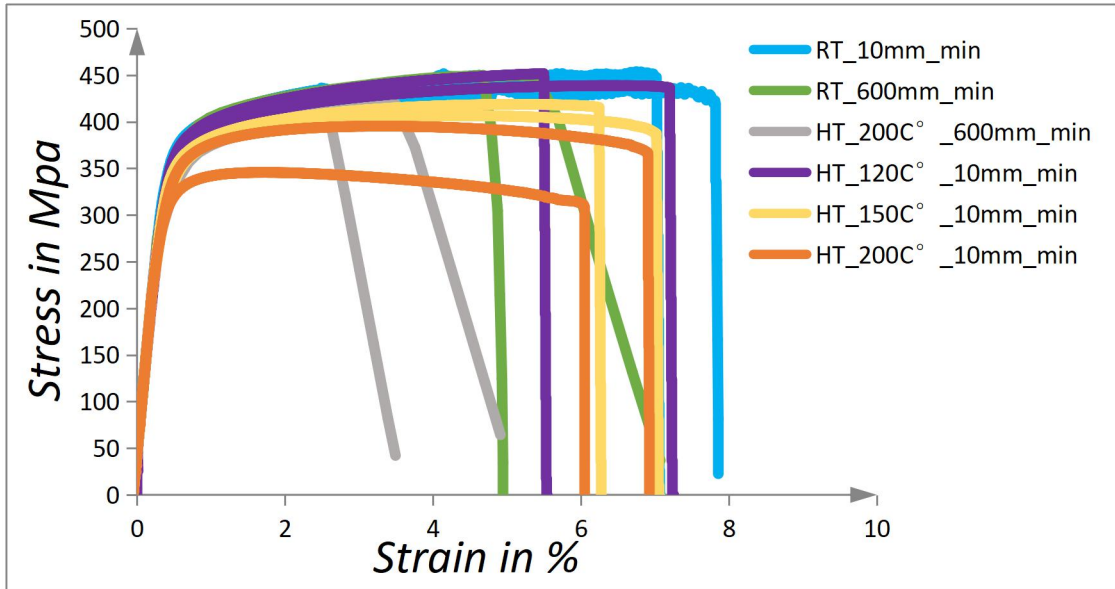


Fig. 17: stress-strain curves of AA5083

Figure 18 shows the stress-strain relationships for deformation at different stretching speeds at the same temperature of 200°C and RT. At room temperature, the UTS at a stretching speed of 10 mm/min is close to that at 600 mm/min; at 200°C, the stress at a stretching speed of 10 mm/min is significantly smaller than that at 600 mm/min. At the same temperature, the ultimate stress value increases with the increase of the stretching speed, but the increase amplitude varies greatly in different cases, and the total elongation decreases significantly with the increase of the stretching speed.

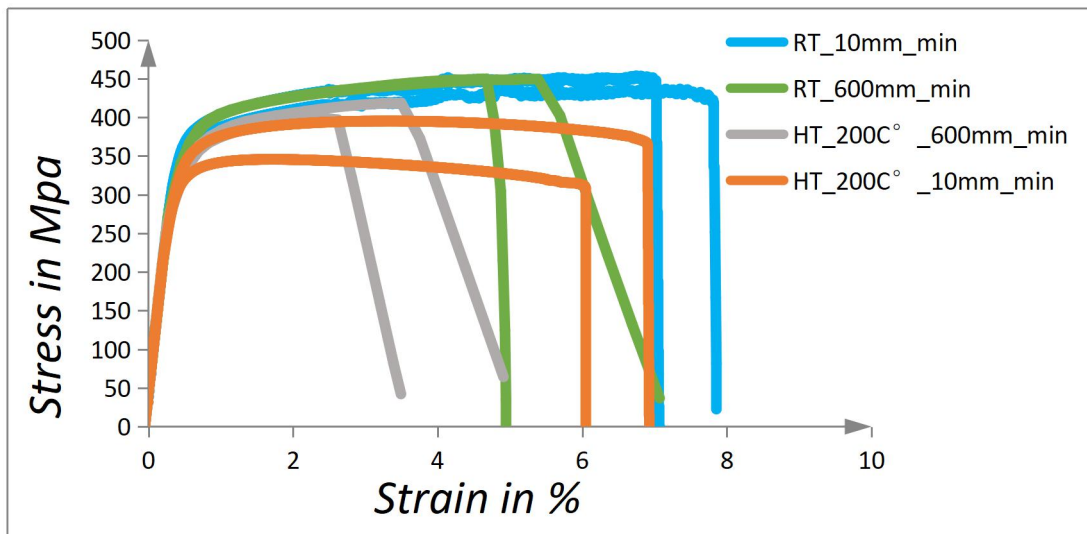


Fig. 18: AA5083 stress-strain curves at same temperature, different tensile speeds.

When AA5083 is in the same tensile speed of 10mm/min, different temperature cases: RT, 120°C, 150°C, 200°C (Fig. 19). We can see that the ultimate tensile stress basically does not change when the temperature rises from RT to 120°C, and the elongation decreases about 1%; when the temperature reaches 150°C and 200°C, the stress decreases significantly, but the average elongation does not change much, which indicates that exposure to this temperature and stretching speed has less effect on the elongation.

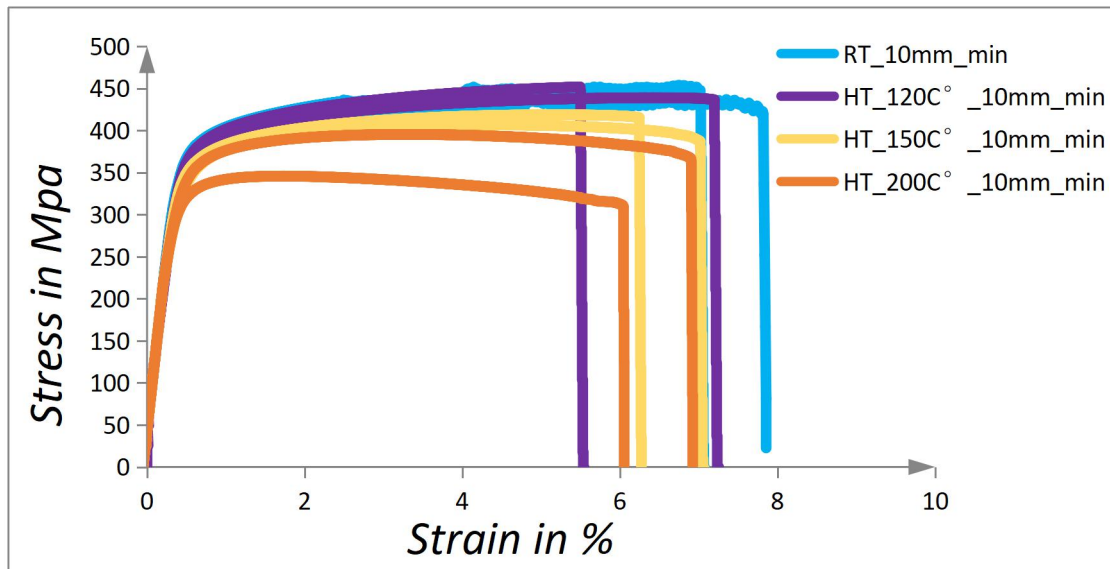


Fig. 19: AA5083 Stress-strain curves are at the same tensile speed, different temperatures.

When AA5083 is stretched at 10 mm/min at room temperature, a distinct "serration" of the stress-strain curve is observed (Fig. 20), which is considered to be the Portevin-Le Chatelier effect (PLC). This effect is also observed on the surface of the specimen and in the plastic deformation zone. The minimum strain required for a sawtooth to appear on the stress-strain curve is called critical strain, and its presence is due to better solute diffusivity resulting from the vacancies created by the deformation and the increased density of mobile dislocations [28]. The "sawtooth" disappeared as the specimen temperature was increased to 120°C, 150°C, 200°C, or by increasing the stretching speed to 600 mm/min, with significant effects of temperature and strain rate.

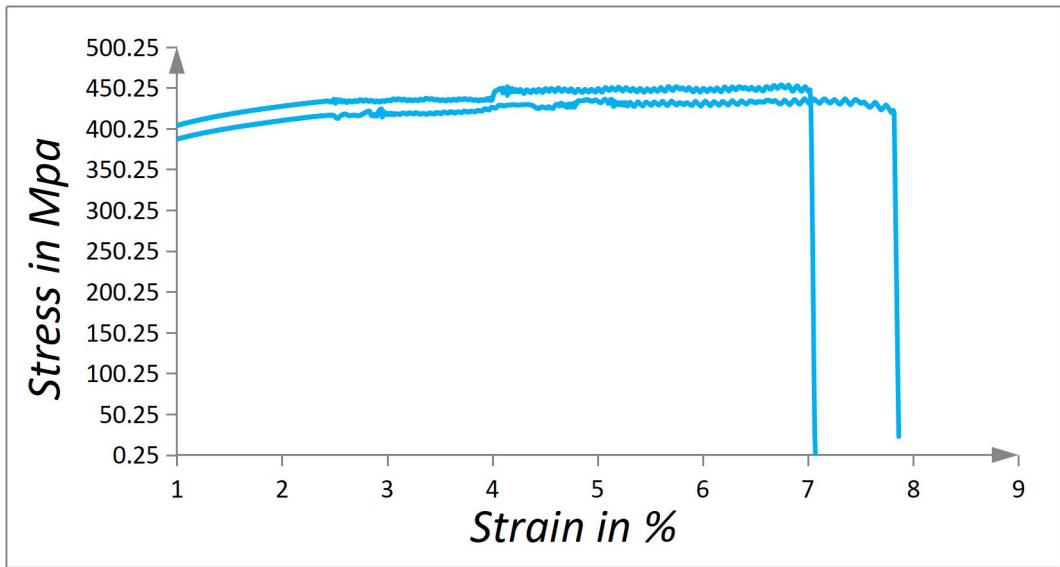


Fig. 20: PLC curves of AA5083 at RT at 10 mm/min.

5.33 Tensile test results for AA7046

A total of 8 tensile tests (stress-strain relationship Fig. 21, relevant data Table 6) were conducted for AA7046 at different temperatures and tensile speeds, as follows:

- 2 tests at RT and 10 mm/min
- 2 tests at RT and 600 mm/min
- 2 tests at 175 °C and 10 mm/min
- 2 tests at 200 °C and 10 mm/min

Alloy 7046 (Average Value)	Ultimate Tensile Strength (MPa)	Yield Strength (MPa)	Uniform Elongation (%)	Elongation At Fracture (%)
RT 10mm/min	370	223	17.6	18.5
RT 600mm/min	354	229	17.3	14.7
175°C 10mm/min	302	194	17.6	21
200°C 10mm/min	288	211	12.3	15.8

Table 6: Main data of AA7046 stress-strain curves

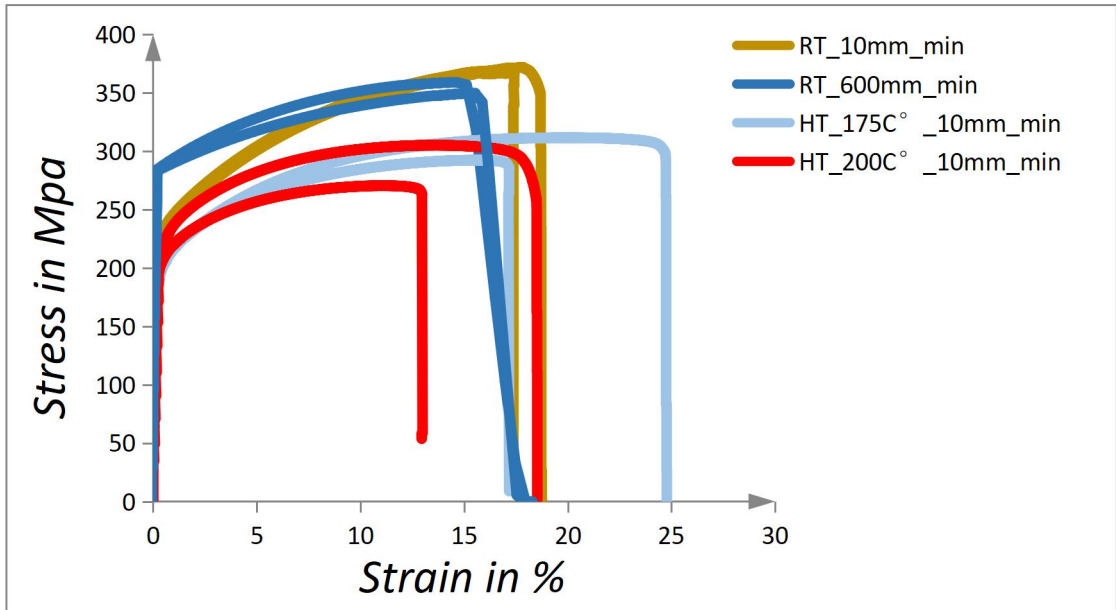


Fig. 21: stress-strain curves of AA7046

As observed in Fig. 22, AA7046 showed high values of ultimate tensile strength (UTS) at room temperature accompanied by tensile speeds of 10 mm/min and 600 mm/min. However, at 600 mm/min tensile speed, the total elongation decreased and the yield strength increased.

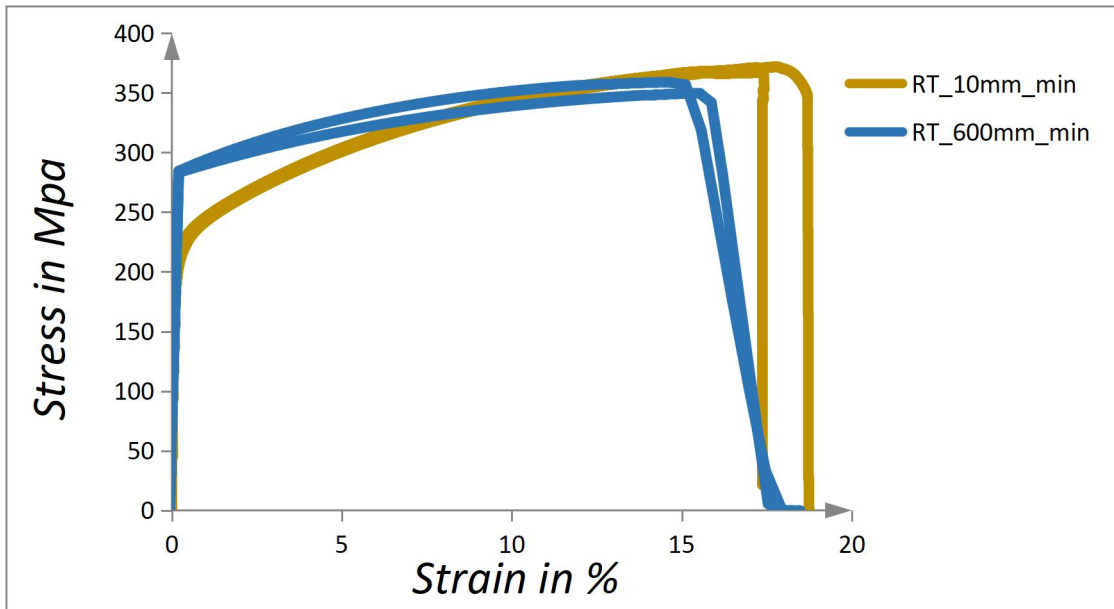


Fig. 22: AA7046 stress-strain curves at same temperature, different tensile speeds.

Fig.23 shows that at the same tensile speed (10 mm/min), at different temperatures, accompanied by an increase in temperature from RT to 175°C, the work hardening decreases with increasing forming temperature, which also corresponds to an increase in total elongation, due to the dispersion of the necking shrinkage preventing the concentration of plastic strain in localized locations; as the temperature continues to increase to 200°C, both strength and total elongation decrease significantly; this indicates that significant changes in mechanical properties are caused at this temperature, most likely due to the dissolution of precipitates, which eliminates the hardened T6 temper.

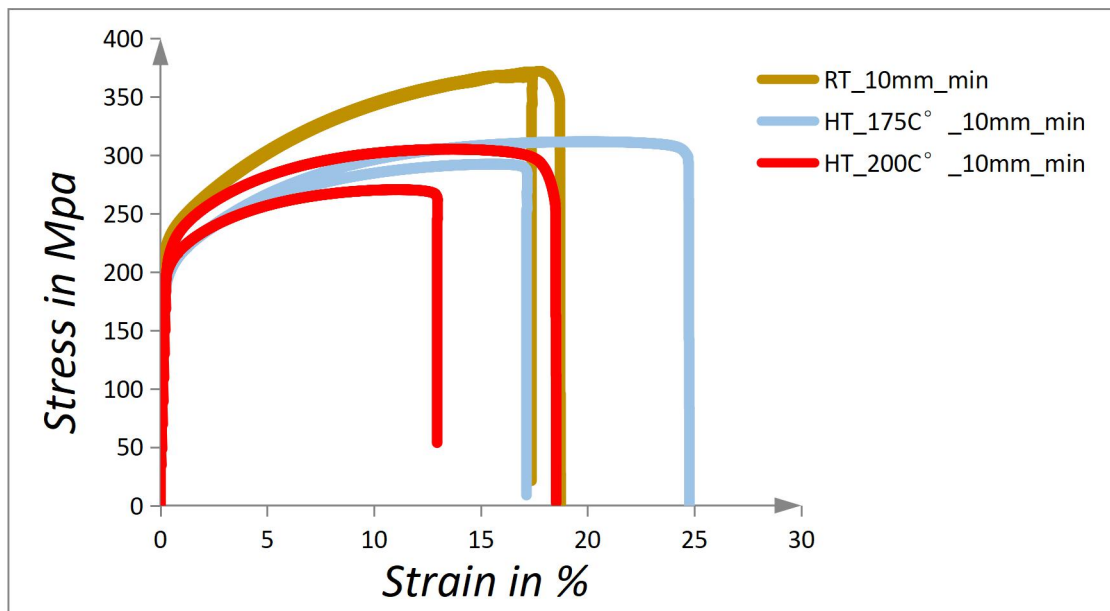


Fig. 23: AA7046 Stress-strain curves are at the same tensile speed, different temperatures

5.34 Observations for broken samples

About all broken samples are shown in Fig. 24, Fig. 25 and Appendix I. We can see that some samples have plastic lips in the fracture and are inclined at an angle of about 45 degrees, which indicates that the shear stress has reached its limit and ductile fracture has occurred. In addition, it can be observed that some fractures show a significant contraction, which is a necking phenomenon due to a large amount of plastic deformation. We also observed some black dots on the fracture surfaces, which are most likely due to the generation of oxidation. Some of these fractures were located at the bottom of the sample, which could be caused by the sample being tilted during clamping or by machining defects in the sample, such as: internal impurities, uneven machining dimensions, etc. We also found that the fracture of sample 5083-RT-600 mm/min (b) had a "peak shape" and a double oblique fracture, which did not occur in sample (a) and was probably caused by the presence of the original notch at the fracture location in sample (b).

				
5083 <i>RT 10mm/ min</i>	5083 <i>RT 600mm/ min(a)</i>	5083 <i>RT 600mm/ min(b)</i>	5083 <i>120°C 10mm/ min(a)</i>	5083 <i>120°C 10mm/ min(b)</i>
				
5083 <i>150°C 10mm/ min(a)</i>	5083 <i>150°C 10mm/ min(b)</i>	5083 <i>200°C 10mm/ min</i>	5083 <i>200°C 600mm/ min(a)</i>	5083 <i>200°C 600mm/ min(b)</i>

Fig. 24: Broken samples for AA5083

7046 RT 10mm/ min(a)	7046 RT 10mm/ min(b)	7046 RT 600mm/ min(a)	7046 RT 600mm/ min(b)	7046 175°C 10mm/ min(a)	7046 175°C 10mm/ min(b)	7046 200°C 10mm/ min(a)	7046 200°C 10mm/ min(b)

Fig. 25: Broken samples for AA7046

5.4 Optical Metallography

5.4.1 Samples preparation

First, we used the following 4 samples as our test subjects and cut them with the TR80 EVOLUTION Abrasive Cutter (Fig. 26).

- 5083-RT, cut from one specimen end, after testing at RT-10 mm/min.
- 5083-200°C, cut from one specimen end, after testing at 200°C-10 mm/min.
- 7046-RT, cut from one specimen end, after testing at RT-10 mm/min.
- 7046-200°C, cut from one specimen end, after testing at 200°C-10 mm/min.



Fig. 26: TR80 EVOLUTION Abrasive Cutter

Then, we put the cut sample into a mold (Fig. 27) and use-Technovit 4071 powder and solution (it is a cold-mounted resin), mix it quickly at room temperature in a 2:1 ratio, pour it into the mold and wait for it to solidify to make the optical microscope (OM) sample in Fig. 27.

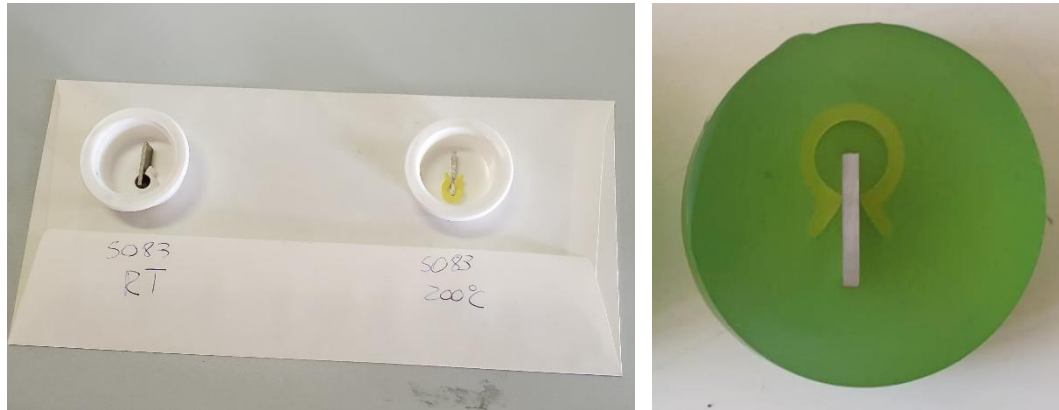


Fig. 27: OM molds and samples

Next, we used a REMET LS 2 polisher and abrasive paper (labeled 80-4000, the larger the number, the smaller the abrasive particles) to gradually polish the OM samples initially and then polish them with a finer cloth and diamond abrasive (3 microns, 1 micron) to produce a mirror-like finish for microscopic observation. Throughout the process we use water (preliminary grinding stage) and lubricant (polishing stage) to carry away the heat and the abraded particles.

Finally, the samples of polished OM were chemically etched in 1% HF, 1.5% HCl, 2.5% HNO₃, 95% H₂O aqueous solution (Keller solution) (AA5083 for about 35s, AA7046 for about 75s), then rinsed with water and dried by hot-air blower.

5.42 Microstruture analysis

The Reichert-Jung optical microscope was used to observe the microstructure of the above four OM samples (5083-RT-10 mm/min, 5083-200°C-10 mm/min, 7046-RT-10 mm/min, 7046-200°C-10 mm/min).

In each sample we arbitrarily selected three different positions for observation. Fig. 28 shows the microscopic views of samples 5083-RT (left) and 5083-200°C-10 mm/min (right) at 20x, 50x, and 100x magnification in the microscope, respectively.

Due to the typed etching, we were not successful in observing the grain boundary, and the precipitates (black dots) are not different between the two.

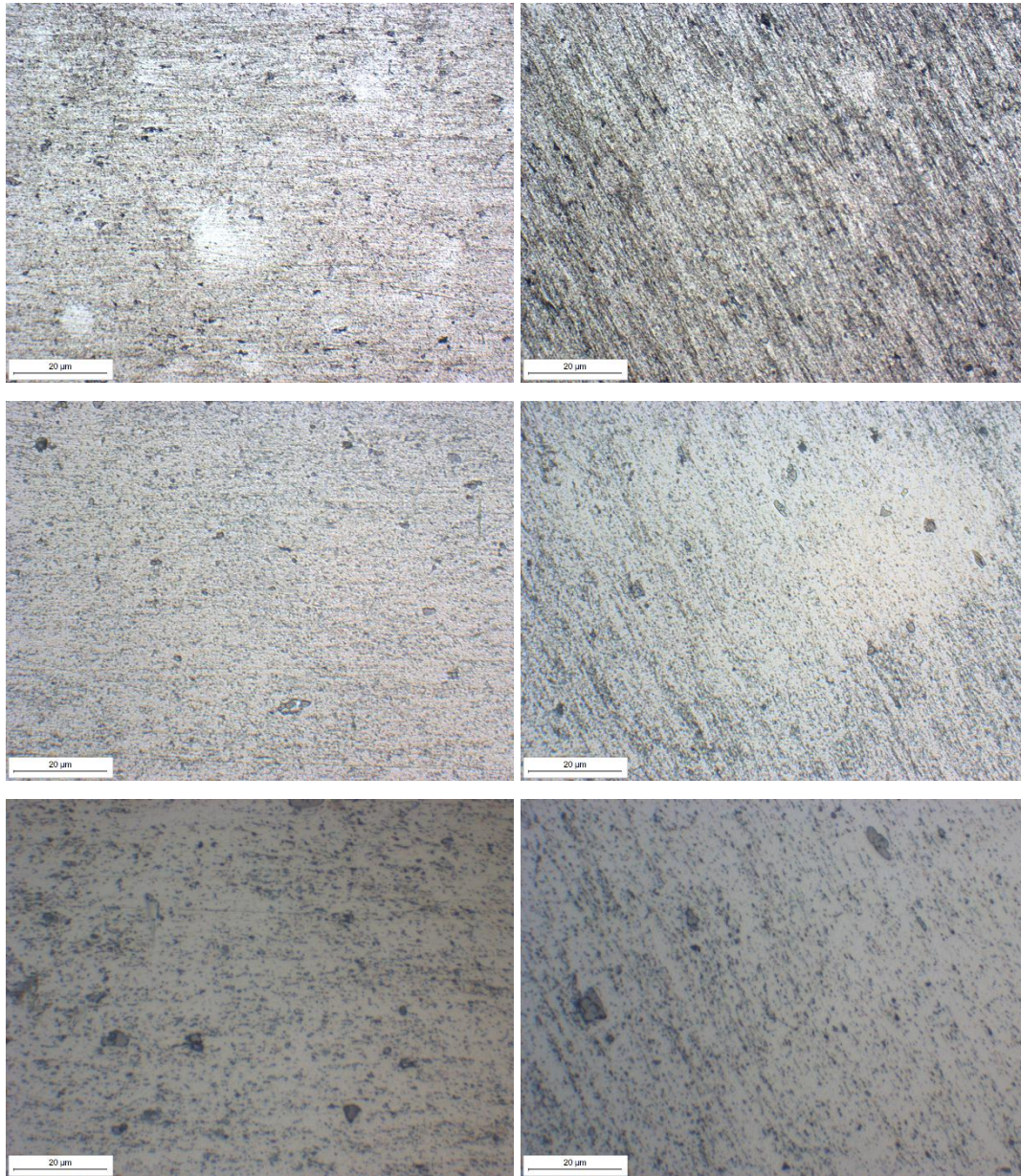


Fig. 28: Microstructures(20x 50x 100x), 5083-RT-10 mm/min(left), 5083-200°C-10 mm/min(right)

Similarly, in each sample of AA7046 we also arbitrarily selected three different positions for observation. Fig. 29 shows the microscopic fields of samples 7046-RT (left) and 7046-200°C-10 mm/min (right) at 20x, 50x and 100x magnification in the microscope, respectively.

Clear distribution of grain boundary and precipitates can be observed in the figure

below, and no significant difference was found between the two. In addition, the grains were not elongated because the test samples were taken at a place where no metal strain occurred.

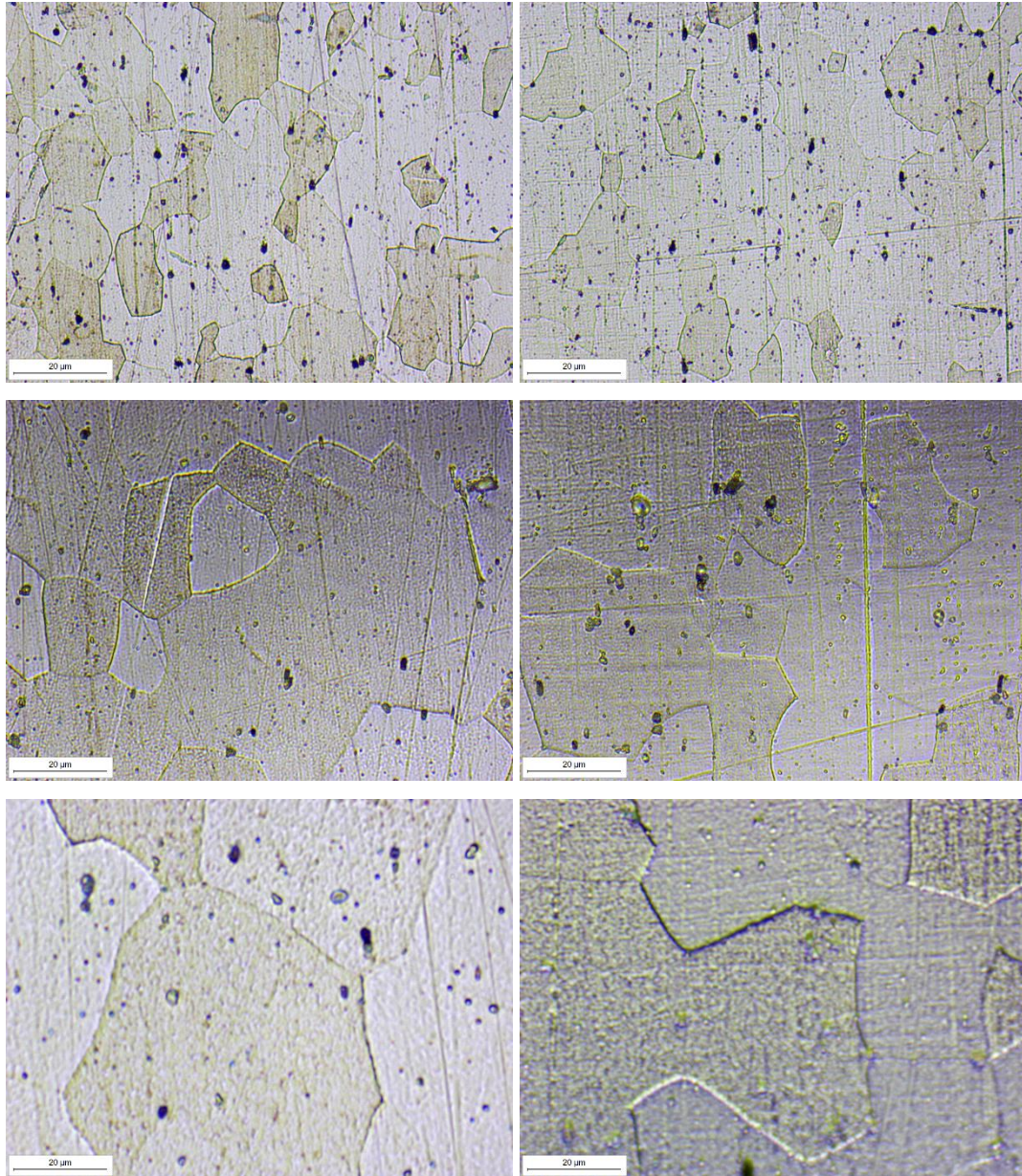


Fig. 29: Microstructures(20x 50x 100x), 7046-RT-10 mm/min(left), 7046-200°C-10 mm/min(right)

5.5 Microhardness tests

5.51 Equipment and principle

Hardness is the ability of a material to resist plastic deformation by pressing into the surface of another harder object, which is one of the important mechanical properties and is widely used in industrial production. The test samples we used this time are 4 samples (5083-RT, 5083-200°C, 7046-RT, 7046-200°C) which have been observed in microstructure before. The test principle is: a diamond prismatic indenter with an angle of 136 degrees between opposite faces (Fig. 30) is pressed into the surface of the sample under a specified load F . The load is removed after holding for a fixed time, the diagonal length d of the indentation is measured, and the surface area of the indentation is calculated, and the average pressure on the surface area of the indentation is calculated, which is the Vickers hardness value of the metal, expressed by the symbol HV.

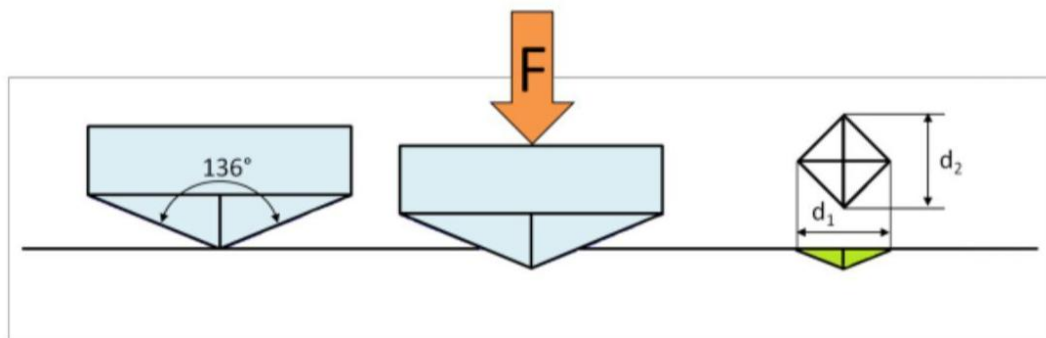
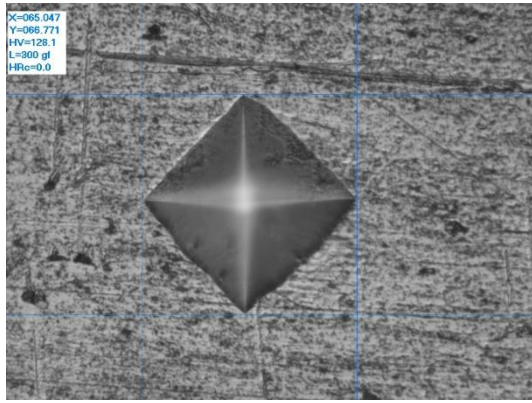
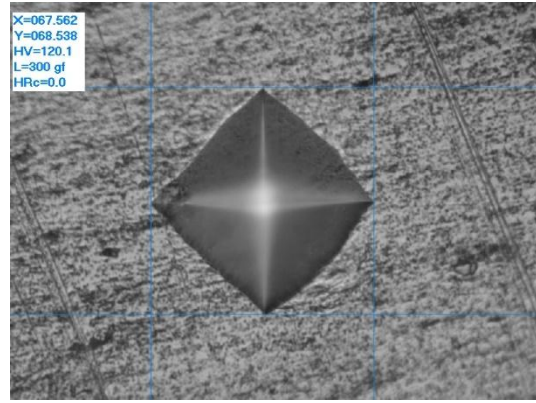


Fig. 30: Diamond ortho-prismatic indenter of Vickers hardness tester and the resulting indentations

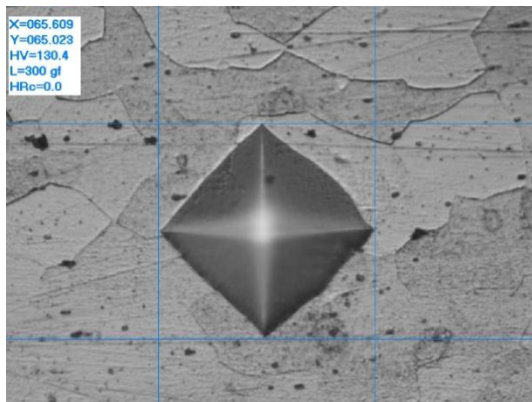
In this work, a load of 2.94N (300gf) was used in all cases, total of 5 indentations were made on each specimen (Fig. 31).



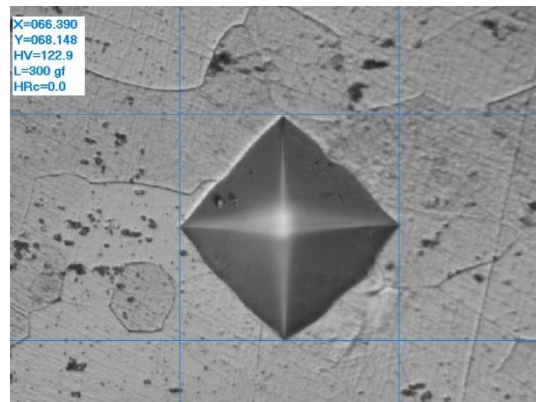
AA5083-RT



AA5083-200°C



AA7046-RT



AA7046-200°C

Fig. 31: Indentations produced on 4 experimental samples

5.52 Data analysis

The hardness test results shown in Table 7 indicate that the Microhardness of AA5083 and AA7046 (after solution and partial aging heat treatment) are similar and decrease with increasing forming temperature, but the decrease is small. From these data, we can conclude that warm forming at this temperature does not affect Microhardness much.

	<i>AVERAGE</i>	<i>ST. DEV.</i>	<i>#1</i>	<i>#2</i>	<i>#3</i>	<i>#4</i>	<i>#5</i>
<i>5083-RT</i>	129	1.6	130.5	128.1	127.7	126.6	129.6
<i>5083-200°C</i>	123	1.7	124.4	124	123.3	120.1	123.7
<i>7046-RT</i>	128	1.8	126.6	129.2	128.5	126.2	130.4
<i>7046-200°C</i>	123	3.1	125.5	126.6	118.8	122.9	121.9

Table 7: Microhardness test data for 4 samples

6. Conclusions

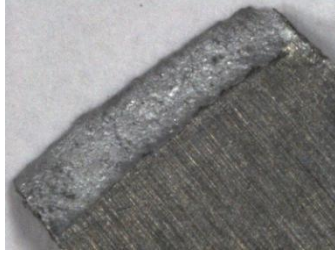
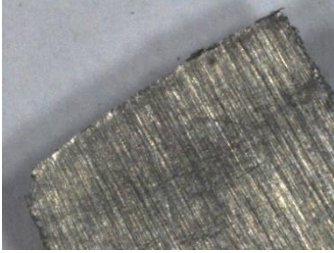
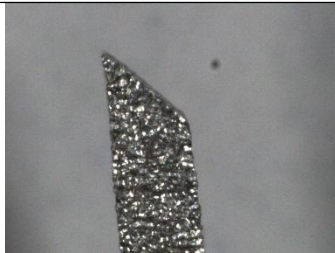
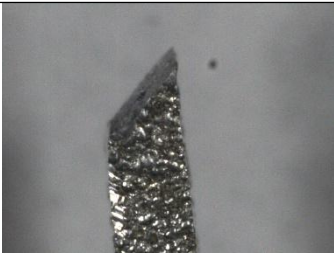
In this study, the mechanical properties of AA5083 and AA7046-T6 aluminum alloys were investigated under different processing conditions, and the following conclusions can be obtained:

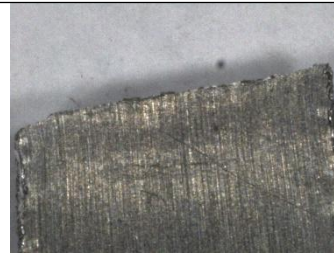
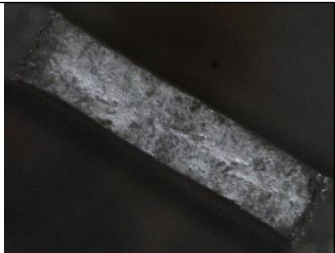
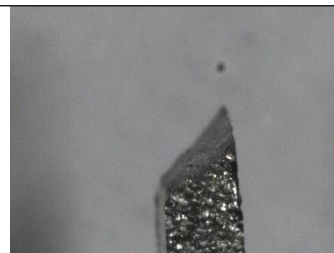
- The results of tensile tests show that the temperature has a small effect on the properties of AA5083 at temperatures below 120°C (10 mm/min). Above this temperature up to 200°C (10mm/min), although the ultimate tensile strength decreases with increasing temperature, the elongation is basically unaffected in this interval. When the tensile speed is increased significantly at room temperature (600mm/min), the ultimate tensile strength is in a stable state. The "PLC" phenomenon occurs at room temperature and at the same time at low stretching speeds, and can be eliminated by increasing the forming temperature and stretching speed.
- However, for AA7046, a large increase in tensile speed at room temperature also has no significant effect on the ultimate tensile strength. In addition, the total elongation does not always decrease with increasing temperature, but peaks at 21% at 175°C, indicating a good ductility at this temperature. At 200°C, it decreases to about 15.8%. On the other hand, the tensile strength decreases gradually with increasing temperature.
- Comparing AA5083 with AA7046, it is found that the ultimate tensile strength of the former is higher than the latter, but the ductility is much lower. The elongation of both alloys decreases significantly with a large increase in tensile speed under all test conditions.
- From the microstructure observation, it was concluded that this warm forming

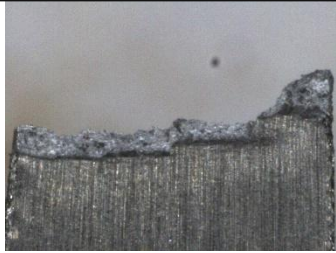
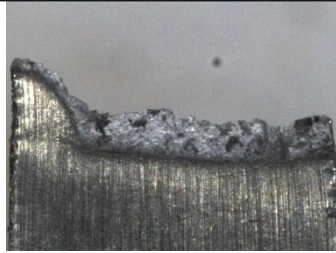
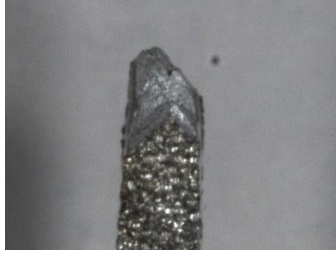
process did not cause significant changes in the morphology and size distribution of grains and precipitates, which may need further exploration.

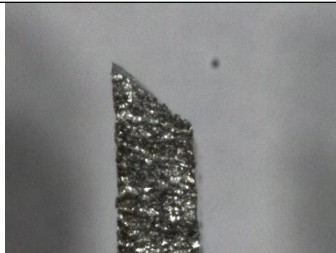
- In the hardness test, the warm forming of AA5083 and AA7046 at 200°C only resulted in a slight decrease in hardness, which indicates that the effect on hardness at this temperature is negligible.

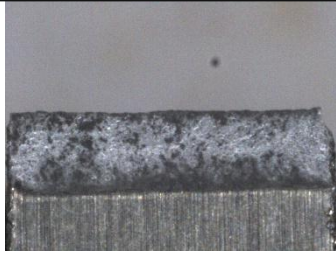
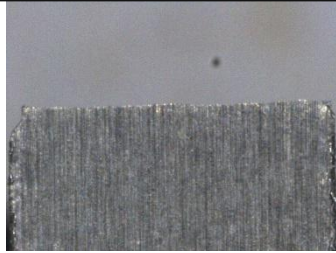
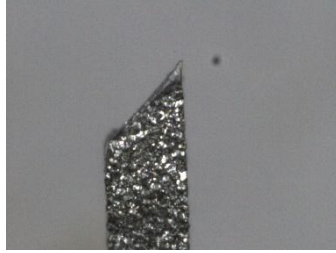
7. Appendix I

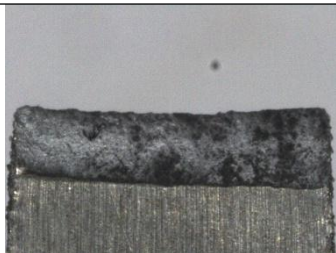
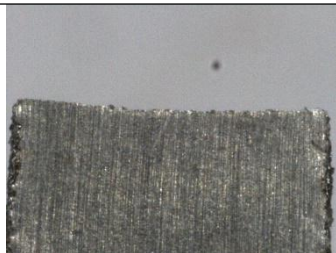
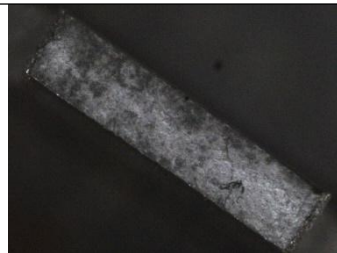
5083 <i>RT</i> 10mm <i>/min</i>			
	Front-1	Front-2	Axial
			
	Side-1, 46°	Side-2, 42°	

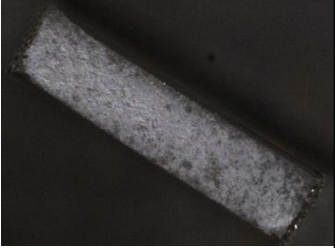
5083 <i>RT</i> 600m <i>m/</i> <i>min</i> <i>(a)</i>			
	Front-1	Front-2	Axial
			
	Side-1, 44°	Side-2, 48°	

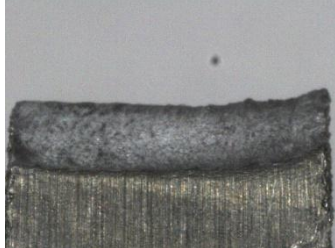
5083 RT 600m m/ min (b)			
	Front-1	Front-2	Axial
			
Side-1	Side-2, 44°		

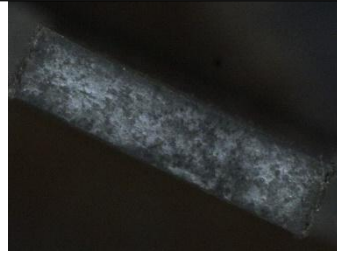
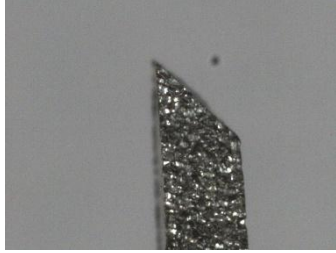
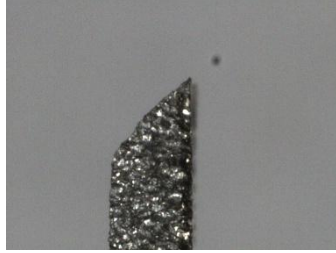
5083 120°C 10mm /min (a)			
	Front-1	Front-2	Axial
			
Side-1, 47°	Side-2, 46°		

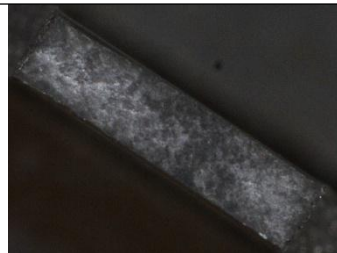
5083 120°C 10mm /min (b)			
	Front-1	Front-2	Axial
			
Side-1, 44°	Side-2, 47°		

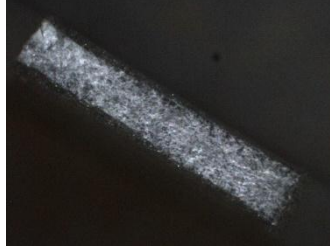
5083 150°C 10mm /min (a)			
	Front-1	Front-2	Axial
			
Side-1, 53°	Side-2, 45°		

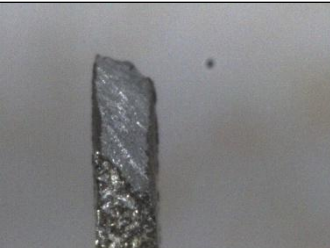
5083 150°C 10mm /min (b)			
	Front-1	Front-2	Axial
			
Side-1, 49°	Side-2, 44°		

5083 200°C 10mm /min			
	Front-1	Front-2	Axial
			
Side-1, 48°	Side-2, 47°		

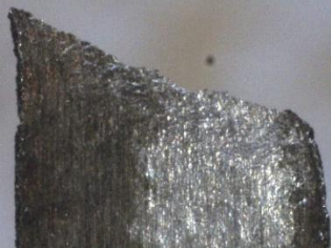
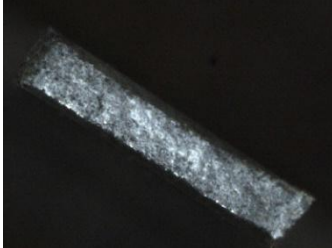
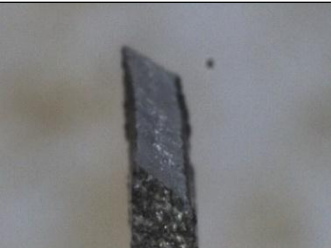
<p>5083 200°C 600m m/ min (a)</p>			
	Front-1	Front-2	Axial
			
	Side-1, 45°	Side-2, 47°	

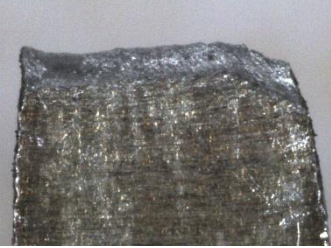
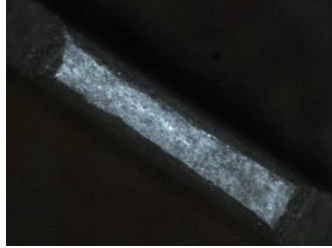
<p>5083 200°C 600m m/ min (b)</p>			
	Front-1	Front-2	Axial
			
	Side-1, 45°	Side-2, 47°	

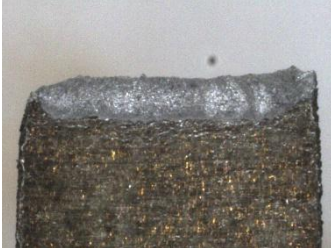
7046 RT 10mm /min (a)			
	Front-1, 52°	Front-2, 60°	Axial
			
	Side-1, 49°	Side-2	

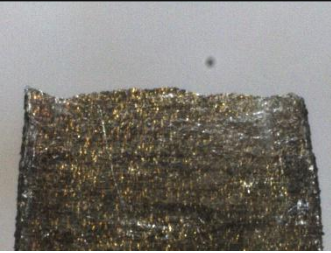
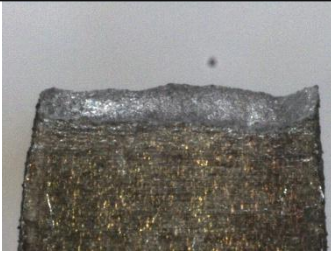
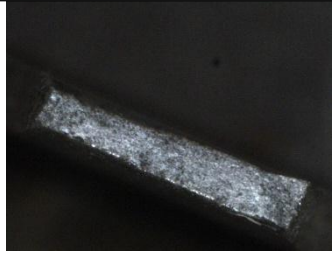
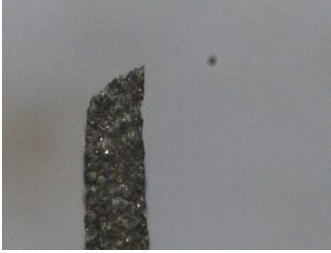
7046 RT 10mm /min (b)			
	Front-1, 67°	Front-2, 64°	Axial
			
	Side-1, 46°	Side-2, 62°	

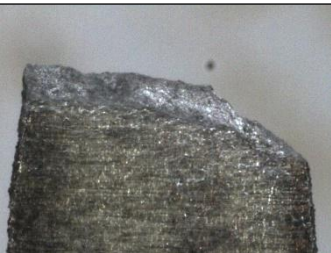
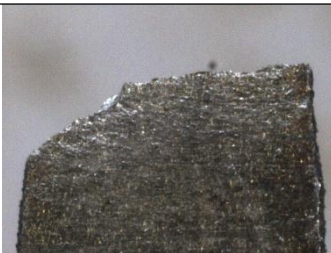
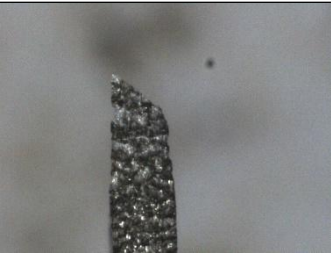
7046 RT 600m <i>m/min</i> (a)			
	Front-1, 70°	Front-2, 75°	Axial
			
	Side-1, 50°	Side-2	

7046 RT 600m <i>m/min</i> (b)			
	Front-1, 66°	Front-2, 68°	Axial
			
	Side-1, 55°	Side-2, 57°	

7046 175°C 10mm /min (a)			
	Front-1	Front-2	Axial
			
	Side-1, 50°	Side-2, 49°	

7046 175°C 10mm /min (b)			
	Front-1	Front-2	Axial
			
	Side-1, 58°	Side-2, 56°	

7046 200°C 10mm /min (a)			
	Front-1	Front-2	Axial
			
	Side-1, 49°	Side-2, 58°	

7046 200°C 10mm /min (b)			
	Front-1	Front-2	Axial
			
	Side-1, 55°	Side-2, 64°	

8. References

- [1]CACERES C H. Economicalandenvironmentalfactorsinlightalloys automotive applications [J] . Metallurgical and Materials Transactions A, 2007,38(7) :1649-1662.
- [2]INGARAO G, LORENZO R D, MICARI F. Sustainabilityissues in sheet metal forming processes: an overview [J] . Journal of Cleaner Production, 2011 ,19(4) :337-347.
- [3]WANG B L, ZENG K. Acceleratingtheinnovation and development ofautomotivelightweight material [J] . Advanced Materials Industry, 2018(10) : 17-19 .
- [4]UACJ Corporation, Japan: uacj-automobile.com
- [5]Mingjun YANG, Kai LI, Yong DU, Jiong WANG, Siliang LIU, Yi KONG. Experimental Characterization of Ultrastructure of Aviation Aluminum Alloys[J]. Journal of Aeronautical Materials, 2017, 37(1): 36-51.
- [6]W. S. Miller, L. Zhuang, J. Bottema, A. J. Wittebrood, P. De Smet, A. Haszler, A. Vieregge, Mater. Sci. Eng. A, vol. 280, no. 1, pp. 37–49, (2000).
- [7]China International Industry Fair, Aluminum alloy heat treatment characteristics, Exhibition News, 2021
- [8]Pat Sooksaen, Onnuch Chulasinont, Paradee Janmat, Wilaiwan Thovasakul, Chemical treatment on aluminum alloy for hydrophobic surfaces, Materials Today: Proceedings, Volume 4, Issue 5, Part 2, 2017,Pages 6528-6533
- [9]YU Z, ZHANG M, SUN B, et al. Aluminium Alloys in Common Use and Their Heat Treatment Process [J][J]. Heat Treatment, 2006, 3.
- [10]Correia, Sergio, Vitor Anes, and Luis Reis. "Effect of Surface Treatment on Adhesively Bonded Aluminium-aluminium Joints regarding Aeronautical Structures." Engineering Failure Analysis 84 (2018): 34-45.
- [11]N.-C. Wu, M.-S. Tsai, M.-C. Wang and H.-S. Liu, "The morphology and formation mechanism of aluminum nitride nanocrystals synthesized by chemical vapor deposition", J. Cryst. Growth, vol. 208, pp. 189-196, Jan. 2000.
- [12]Z. Y. Fan, G. Rong, J. Browning and N. Newman, "High temperature growth of

AlN by plasma-enhanced molecular beam epitaxy", Mater. Sci. Eng. B, vol. 67, pp. 80-87, Dec. 1999.

[13]W. Wang, H. Qian, W. Yang, H. Wang, Y. Zhu and G. Li, "Effect of Al substrate nitridation on the properties of AlN films grown by pulsed laser deposition and its mechanism", J. Alloys Compound, vol. 644, pp. 444-449, Sep. 2015.

[14]C.-T. Chang, Y.-C. Yang, J.-W. Lee and B.-S. Lou, "The influence of deposition parameters on the structure and properties of aluminum nitride coatings deposited by high power impulse magnetron sputtering", Thin Solid Films, vol. 572, pp. 161-168, Dec. 2014.

[15]X. Nie, A. Leyland, A. L. Yerokhin, H. W. Song, S. J. Dowey and A. Matthews, "Thickness effects on the mechanical properties of micro-arc discharge oxide coatings on aluminium alloys", Surf. Coat. Technol., vol. 116, pp. 1055-1060, Sep. 1999.

[16] Aluminum Association's Welding Aluminum Theory and Practice and American Welding Society Document D1.2 – Structural Welding Code – Aluminum

[17]Shriwas A K, Kale V C. Impact of aluminum alloys and microstructures on engineering propertiesreview[J]. IOSR Journal of Mechanical and Civil Engineering, 2016, 13(3): 16-22

[18]P.J Bolt, N.A.P.M Lamboo, P.J.C.M Rozier, Feasibility of warm drawing of aluminium products, Journal of Materials Processing Technology, Volume 115, Issue 1,2001,Pages 118-121

[19]Palaniswamy, H., et al. "New Technologies to Form Light Weight Automotive Components." Proceedings of 4th International Conference and Exhibition on Design and Manufacturing of Machines and Dies/Molds, June. 2007.

[20]National Machinery Company, www.nationalmachinery.com

[21]Altan, Taylan, and A. Erman Tekkaya, eds. Sheet metal forming: processes and applications. ASM international, 2012.

[22]Dröder, Klaus Georg: Untersuchungen zum Umformen von Feinblechen aus Magnesiumknetlegierungen. University of Hannover, Dec.1999

[23]D. Li and A.K. Ghosh, Biaxial Warm Forming Behavior of Aluminum Sheet

- Alloys, *J. Mater. Process. Technol.*, Vol 145, 2004, p 281–293
- [24]M. Bauccio et al., Ed., *ASM Metals Reference Book*, 3rd ed., ASM International, 1993
- [25]S. Kaya, G. Spampinato, and T. Altan, An Experimental Study on Non-Isothermal Deep Drawing Process Using Aluminum and Magnesium Alloys, *J. Manuf. Sci. Eng. (Trans. ASME)*, Vol 130, 2008
- [26]H. Takuda, K. Mori, I. Masuda, Y. Abe, and M. Matsuo, Finite Element Simulation of Warm Deep Drawing of Aluminum Alloy Sheet when Accounting for Heat Conduction, *J. Mater. Process. Technol.*, Vol 146, 2002, p 52–60
- [27]Maillard, A., C. Piat, and YM Chen. "Assessment of Solutions to Reduce Wear with the Warm Forming of Aluminum." *IOP Conference Series. Materials Science and Engineering* 651.1 (2019): 12068. Web.
- [28]Abadi, M., Hahner, P., Zeghloul, A.(2002) "On the characteristic of Portevin-Le Chatelier band in aluminum alloy 5182 under stress controlled and strain- controlled tensile testing" *Materials Science and Engineering A337*: 194–201
- [29]Information provided by The Aluminum Association, Inc. from *Aluminum Standards and Data 2000 and/or International Alloy Designations and Chemical Composition Limits for Wrought Aluminum and Wrought Aluminum Alloys (Revised 2001)*.
- [30]Laurent H *et al* 2011 Mechanical behaviour and springback study of an aluminium alloy in warm forming conditions *ISRN Mechanical Engineering* 1–9
- [31]Wikipedia, the free encyclopedia, https://en.wikipedia.org/wiki/Motor_vehicle